Optimum Aggregation and Control of Spatially Distributed Flexible Resources in Smart Grid

Bhattarai, Bishnu Prasad; Mendaza, Iker Diaz de Cerio; Myers, Kurt S.; Bak-Jensen, Birgitte; Paudyal, Sumit

Published in:
I E E E Transactions on Smart Grid

DOI (link to publication from Publisher):
10.1109/TSG.2017.2686873

Publication date:
2018

Document Version
Accepted author manuscript, peer reviewed version

This article has been accepted for publication in a future issue of this journal, but has not been fully edited. Content may change prior to final publication. Citation information: DOI 10.1109/TSG.2017.2686873, IEEE Transactions on Smart Grid

Optimum Aggregation and Control of Spatially Distributed Flexible Resources in Smart Grid

Bishnu P. Bhattarai[1], Iker Diaz de Cerio Mendaza[2], Kurt S. Myers[1], Brigitte Bak-Jensen[3], and Sumit Paudyal[4]
[1]Department of Power and Energy System, Idaho National Laboratory, Idaho, USA;
[2]Department of System Planning, Energinet.dk, Fredericia, Denmark;
[3]Department of Energy Technology, Aalborg University, Aalborg, Denmark;
[4]Department of Electrical Engineering, Michigan Technological University, Michigan, USA
Corresponding Email: *Bishnu.Bhattarai@inl.gov*

***Abstract*—This study presents an algorithm to optimally aggregate spatially distributed flexible resources at strategic microgrid/smart-grid locations. The aggregation reduces a distribution network having thousands of nodes to an equivalent network with a few aggregated nodes, thereby enabling distribution system operators (DSOs) to make faster operational decisions. Moreover, the aggregation enables flexibility from small distributed flexible resources to be traded to different power and energy markets. A hierarchical control architecture comprising a combination of centralized and decentralized control approaches is proposed to practically deploy the aggregated flexibility. The proposed method serves as a great operational tool for DSOs to decide the exact amount of required flexibilities from different network section(s) for solving grid constraint violations. The effectiveness of the proposed method is demonstrated through simulation of three operational scenarios in a real low voltage distribution system having high penetrations of electric vehicles and heat pumps. The simulation results demonstrated that the aggregation helps DSOs not only in taking faster operational decisions, but also in effectively utilizing the available flexibility.**

***Index Terms*—Demand aggregation, demand flexibility, demand response, electricity market, hierarchical control, smart grid**

I. Introduction

Recently, integration of new electrical loads, such as electric vehicles (EV) and heat pumps (HPs), to the existing grids is increasing rapidly [1]-[2]. As most of the existing grids were not designed to host such sizable loads, they may congest and require costly grid reinforcements. However, sizable ratings provided with energy storage capabilities of EVs and HPs provide significant opportunities to avoid or defer the need of grid reinforcements. More importantly, those flexible resources can be utilized for various grid supports, such as peak shaving and load shifting [3], grid constraints violations management [4], frequency regulation [5], system balancing [6]. Various control algorithms and strategies (e.g., optimal scheduling [7]-[8], coordinated control [9], real-time price based control [10], adaptive control [11]) have been developed for enabling flexible resources for aforementioned grid supports. Nonetheless, despite those technical progresses, consumer acceptance is being one of the potential challenges in practical deployment of those approaches [12].

The consumer acceptance can be addressed by providing enough financial benefits in return to their offer of flexibilities. This requires participation of flexibilities to different electricity markets for maximizing consumer benefits. However, as illustrated in [13],[14], the market participation of small and spatially distributed resources is challenged by increased complexities, economy of scale, need of costly dedicated communication framework, and high errors associated with the forecast of individual consumer flexibility [15]. In addition to those technical complexities, several regulatory issues (e.g., minimum block of time and size) also prohibit easy trade of the flexibility from small distributed resources [16].

Participation of flexible resources to multiple electricity markets can be ensured by developing proper aggregation approaches. Increased financial benefits resulting from multiple market participation increases the utilization of currently untapped flexibility [17], [18]. The aggregation also improves forecasting accuracy and reduces complexities in network computations [19], [20]. The aggregation of flexible resources (e.g., EVs , thermostatic loads) is widely discussed in the recent literature [21]-[28]. The authors in [21], [22] present a mechanism to define demand flexibility and discussed existing load aggregation methods (e.g., bottom up, coordinated, and bus-split). However, these techniques are based on the conventional approach of load aggregation, which cannot be directly implemented to aggregate flexibility. The authors in [23]-[24] present aggregation of flexibility from specific load types, thermostatic loads, using a given demand response (DR) model, in [25], [26] present a fast distributed aggregation techniques with consideration of different payment functions and DR models. In addition, the optimal participation of aggregated DR in wholesale market is investigated in [27], and the impact of uncertainties resulting from DR aggregation to system reliability is investigated in [28]. Nevertheless, these aggregation techniques, which are based on pre-defined DR models and cost-functions, are normally suitable for high level resource planning, but often neglect the spatial distribution of flexibility within the network, operational constraints of individual flexible resources, and local grid constraints.

Moreover, there are various control schemes (e.g., centralized, decentralized, centralized-decentralized, hierarchical) which are widely been used for deploying flexibilities stemming from distributed resources [29]-[35]. Due to better network visibility, the centralized control is often used to establish coordinated control of multiple resources [29]-[30], whereas

This article has been accepted for publication in a future issue of this journal, but has not been fully edited. Content may change prior to final publication. Citation information: DOI 10.1109/TSG.2017.2686873, IEEE Transactions on Smart Grid

the decentralized control is used to realize faster response [31]-[32]. Therefore, a combination of the centralized and decentralized control schemes is implemented to get benefit from both scheme [33]-[34]. However, geographical aspects of the flexibilities, which play a key role in the performance of the local distribution network, are not well integrated in the current control architecture of flexibility utilization. We propose a combination of centralized and decentralized control scheme to effectively deploy the aggregated flexibility. In particular, a distributed control scheme (DCS) exploits demand flexibilities from aggregated areas in the network to solve the local grid constraints, whereas a centralized control scheme (CCS) provides supervisory control and coordination among all DCSs. In addition, CCS can activate flexibilities for supporting upstream grid issues by interfacing with the system operators and electricity markets. This study implements a hierarchical control architecture (HCA) to establish coordinated control and interaction between CCS and DCSs.

The proposed aggregation plays a key role in future grids where millions of active nodes are anticipated due to increased penetrations of solar photovoltaic, EVs, and HPs. More importantly, such resource aggregation significantly reduces the number of active nodes, thereby facilitating distribution system operators (DSOs) for taking faster near real-time operational decisions [36]-[37]. The DSOs can also use aggregation to make better operational planning through understanding of time, amount, and location of available flexibility in the system [41]. The key scientific contributions of this study include:

1) An optimum aggregation algorithm is developed to aggregate spatially distributed flexible resources by considering geographical sparsity of loads and cost of aggregation.
2) Distribution network having large number of nodes is reduced to an equivalent network having a few aggregated loads, and the performance of the aggregated network is compared with the original network for three operating scenarios.
3) A combination of CCS and DCS scheme is designed such that the DCS is implemented at each aggregation point to resolve local grid constraints while the CCS is used to ensure coordination among the DCSs to solve the network level grid requirements.
4) A HCA is designed and implemented to establish control and coordination among CCS and DCSs, and to effectively deploy aggregated demand flexibility for solving grid violations and market participation.

The remainder of this paper is structured as follows. A detailed algorithm to compute optimum aggregation areas for a given distribution network is presented in Section II. Implementation of a HCA is detailed in Section III. Section IV provides comprehensive performance analysis of the proposed algorithm and the paper concludes in Section V.

II. Optimum Aggregation and Network Reduction

Accurate and reliable aggregation of demand flexibility is one of the key need for the future grids to facilitate market participation of small distributed flexible resources and support better and faster operational decisions for DSOs. However, the aggregation of demand flexibility of residential consumer is challenged by the presence of large number of spatially distributed, low-rated devices each having different operational and consumer comfort constraints. One of the effective solutions to handle such resources is to optimally divide the given networks into several areas such that demand flexibilities within each area can be better estimated by a local aggregator assigned to it. Such approach not only facilitates the small distributed consumers for participation to energy markets, but also helps the DSOs to make better operational decisions regarding location, timing, and amount of flexibility needed during a given grid issue.

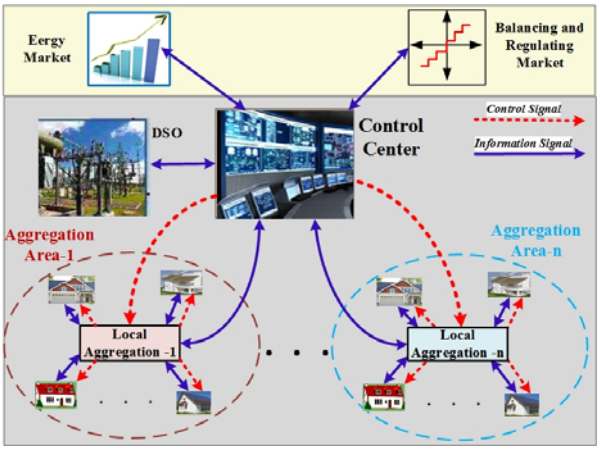

Fig. 1. Schematic diagram of implementation of proposed method.

The overall framework on which the proposed aggregation method works is depicted in Fig. 1. One of the key ideas of the aggregation is to divide a large network into number of local aggregation points such that each local aggregator has better visibility of the flexible resources within its area. Each aggregator collects operational information of flexible resources and makes control decision based on the observed local grid problems (e.g., voltage limit violations), information from energy market (e.g., energy, regulation, balancing) or control information received from DSO/TSO for technical supports to the upstream grids. Nevertheless, computation of optimal aggregation areas and network reductions, utilizing the information from local aggregators to make faster and better operational decisions are key challenges to realize the proposed concept. The following subsections detail the proposed algorithm to determine optimum number of aggregation areas and strategic location for each area so as to aggregate spatially distributed flexible resources.

A. Computation of Optimum Aggregation Areas

Computation of optimum number of aggregation areas (e.g., Area-1, ...Area-n) and corresponding strategic points, as illustrated in Fig. 1, for aggregating the flexible resources of each area is the key aspect of this study. The aggregation

This article has been accepted for publication in a future issue of this journal, but has not been fully edited. Content may change prior to final publication. Citation information: DOI 10.1109/TSG.2017.2686873, IEEE Transactions on Smart Grid

of spatially distributed resources depends greatly on spatial distribution of consumers, cost associated with aggregation (e.g., installation of aggregation point, communication infrastructure), regulatory legislation imposed from contemporary electricity markets (e.g., minimum size and time commitment of flexibility). It should be noted the regulatory legislation for different electricity markets (e.g., day-ahead, balancing, regulating) are different and also vary significantly from one market to the other. To make the proposed methodology more generic, this study focused on spatial distribution of consumers in the network and cost of aggregation to compute optimum aggregation areas as follows:

$$Min. \underbrace{\sum_{i=1}^{N_d}\sum_{j=1}^{N_d} B_{ij}x_{ij} + b_i d_{iT}} + \underbrace{\sum_{i=1}^{N_d} b_i(IC_i^A + OC_i^A)} \quad (1)$$

where x_{ij} is the distance from the j^{th} node to the i^{th} aggregation node, d_{iT} is the distance from the control center to the i^{th} agregation node, b_i is the binary decision variable describing the presence or absence of aggregation point at i^{th} node, and N_d is the total number of nodes in the given feeder. In addition, IC_i^A and OC_i^A are the operating and installation costs associated with the aggregation point at the i^{th} node. Moreover, B_{ij} is a factor which is expressed in terms of decision variable b_i as follows:

$$B_{ij} = b_i(1 - b_{i\pm1})...(1 - b_j) \quad (2)$$

If any node along the path from i^{th} to j^{th} has an aggregation point, B_{ij} become zero, thereby making the product $B_{ij}.x_{ij}$ zero. It is worth mentioning that B_{ij} is not a distance, but helps to compute the nearest distance from i^{th} aggregation node to the j^{th} in combination with x_{ij}. This study assumes nodes are the only candidate locations for the aggregation point. Therefore, both x_{ij} and d_{iT} can be assumed constant for the given network. In particular, x_{ij}, a distances from the i^{th} aggregation node to the j^{th} node, can be written in matrix from as follows:

$$X_{ij} = \begin{bmatrix} x_{11} & \dots & x_{1n} \\ . & \dots & . \\ . & \dots & . \\ x_{n1} & \dots & x_{nn} \end{bmatrix} \quad (3)$$

while d_{iT}, the distance from the central aggregation to the i^{th} node, can be expressed as:

$$D_T = [d_{1T}, ..., d_{nT}] \quad (4)$$

Those distances, d_{iT}, depend primarily on the network topology and spatial distribution of consumers and can be assumed to be constant for a given network. The first part of (1) minimizes the total distance from central aggregation point to individual consumers, while the second part is designed to minimize the total cost of aggregation. As the objective function contains different units (e.g., the first part is distance while the second part is cost), it is normalized as follows:

$$Min. \left(\frac{w_1.f_1(b_i, X_{ij}, Y_{iT})}{D_{Max}} + \frac{w_2.f_2(b_i, IC^A, OC^A)}{N_{Max}.(IC^A + OC^A)} \right) \quad (5)$$

where $f_1(b_i, X_{ij}, Y_{iT})$ and $f_2(b_i, IC^A, OC^A)$ correspond to the first and the second parts of (1), w_1 and w_2 are the weightage assigned to the first and the second parts of (1). In particular, w_1 and w_2 are associated with minimization of distance and total cost of aggregation, respectively. Therefore, assignment of those values solely depends on DSO's preference, for instance, if DSO gives more preference on the minimization of cost, w_2 should be higher than w_1, whereas if DSO is concerned more on better approximation of flexibility by minimizing the aggregation size, w_1 should be higher than w_2. Moreover, D_{Max} is a distance used to normalize the first part of the objective function (i.e., $f_1(b_i, X_{ij}, Y_{iT})$), whereas N_{Max} is used to normalize the second part of the objective function (i.e., $f_2(b_i, X_{ij}, Y_{iT})$). In particular, D_{Max} is the maximum possible distance for the given system which occur when there is no aggregation at all, and the central aggregator is responsible to reach directly to each consumer. Therefore, this is simply obtained by summing D_T.

Similarly, N_{Max} is the maximum possible number of aggregation points in the network, which will be the case when each node is an aggregation point itself. Therefore, N_{Max} will simply be equal to the total number of nodes in the given network. Any preferences/limitations from DSOs, such as total number of aggregation points, maximum possible distance for each aggregation area, can be added in the form of constraints as follows:

$$B_{ij}.x_{ij} \leq \alpha \quad (6)$$

$$\sum b_i \leq N_{Max} \quad (7)$$

where α is the maximum possible distance of consumer from the aggregation point. This is often limited by geographical sparsity as well as DSO's limitations associated with investment on communication infrastructure. Moreover, the constraint (7) limits the number of aggregation point in the given network. This can be obtained or associated with electric utility's investment plans. The optimization problem is solved using the Genetic Algorithm (GA) available in the optimization toolbox of the MATLAB to compute the optimum areas and corresponding strategic locations for aggregating flexible resources in a network. Note that GA is used for taking planning decision for computation of optimum aggregation points, and hence has less concern on computation time unlike in the case of real-time operational planning. We chose GA primarily due to a) ease of implementation, which can be treated as a black box approach despite the size of the network, b) we have observed that the state-of-the-art MINLP solvers (e.g., KNITRO, BARON) also failed for solving large scale MINLP models [38], and often times failed to yield even feasible solutions, and c) GA provides reasonably good solutions and it is easy to obtain feasible solution from GA for

This article has been accepted for publication in a future issue of this journal, but has not been fully edited. Content may change prior to final publication. Citation information: DOI 10.1109/TSG.2017.2686873, IEEE Transactions on Smart Grid

offline problems. Moreover, GA is a better tool for exploring the search space for global optima especially in case of big and highly non-linear problems.

B. Computation of Equivalent Aggregated Network

After computation of the optimum aggregation areas, flexible resources at each area needs to be aggregated to the respective strategic location obtained from Section II-A. In particular, the aggregated load and equivalent impedance to the upstream and downstream connecting nodes should be computed for each aggregation area. It is worth mentioning that the consumer loads dynamically vary over time. As such, both the aggregated load and equivalent impedances are function of time. To deal with such scenario, power consumption of the given network is first clustered into a reasonable number of clusters (N_c) which are then used to compute equivalent impedances.

1) Demand Clustering: Linear clustering techniques such as hierarchical clustering or K-means provides a simple and effective solution to group given set of data into a given number of clusters [39]. Therefore, a hierarchical clustering technique is implemented in this study as an simple and effective technique to cluster hourly time-series power consumption data into predefined number of clusters, N_c. Unlike Mean-shift clustering and Kohonen self-organizing map which require visual inspection to determine the cluster, the hierarchical clustering provides unsupervised clustering of data into the given number of clusters [40]. As the key intent of demand clustering is to compute equivalent impedance for the purpose of determining equivalent aggregated network, linear clusters based on the time-series load data is sufficient for this study. Particularly, the following steps, as proposed in our previous work [41], are implemented to cluster the given set of data.

1) Compute distances among clusters assuming every data set as a cluster of its own.
2) Find the closest distance between a pair of clusters and merge them into a single cluster, so that the number of clusters is reduced by one.
3) Compute the distance between the new cluster and the remaining old clusters, and repeat 2 and 3 until data are clustered into given N_c.

The distance between the pairs of clusters, which is basically the difference between the power demand of two clusters, is computed using a complete-link distance approach, whereby the distance between the clusters P_i and P_j (i.e., $d(P_i, P_j)$) is computed as:

$$d(P_i, P_j) = \max_{p_i \in P_i, p_j \in P_j} \|p_i - p_j\|^2 \tag{8}$$

where p_i and p_j are data of clusters P_i and P_j, respectively. The clustering of time-series data is of key importance to reflect daily and/or seasonal variations on load. Those variations occur in the form of difference in power consumption and in turn will be reflected in the form of changes in the equivalent impedance of each aggregation area. It is worth mentioning that the proposed clustering separates the data based on the hourly demand of the consumer and does not explicitly consider other electrical characteristics (e.g., periodicity, trend, seasonality, consumer behavior). As such, any daily or seasonal variations are reflected only in terms of the variations in the load demand. The details of the proposed hierarchical clustering including its implementation is detailed in our previous work [41].

2) Network Reduction: Following the clustering, loads at each node in a given aggregation area are converted to impedances as follows:

$$Z_i^D = \frac{(V_i^{POC})^2}{P_i^D} \tag{9}$$

where Z_i^D is the load impedance, P_i^D is the power, and V_i^{POC} is the voltage at the point of connection (POC) at i^{th} node, respectively. In order to minimize errors which may be introduced due to assumption of constant impedance load in (9), power flow is performed for the given network using the clustered power to compute V_i^{POC}. This better estimates Z_i^D from the clustered power of each node. After converting all the loads to corresponding impedances, a simple circuit reduction techniques (e.g., series-parallel reduction, $\Pi - T$ transformation) is implemented to compute an aggregated load and an equivalent impedance at the given aggregation point. Finally, the aggregated load impedance at each strategic point is converted back to power using reverse calculation as of (9).

It is worth mentioning that loads are assumed to be constant impedance for the purpose of converting them into an equivalent impedance. Even though this assumption may not be entirely true, errors associated with the constant impedance load assumptions for small ranges of voltage variations are normally lower than errors associated with clustering assumptions and load forecasting [42]. Furthermore, as we also back calculate the load impedance at the aggregation point to an equivalent power by using inverse calculation as (9), the approximation error can greatly be compensated each other. The errors associated with this assumption is relatively small as can be seen from Fig. 9 where the performance of the aggregated network is observed to be very close to the performance of the detailed one.

III. Proposed Control Architecture

This study proposes the HCA which incorporates both centralized and decentralized control philosophies for executing controls of aggregated demand flexibilities. Fig. 2 illustrates a schematic representation of the proposed architecture, whereby a distributed DCS is assigned to each aggregated area and a CCS is assigned to a central control to supervise and coordinate the actions of all DCSs. The key intent of the DCS is to activate flexible demands of the respective aggregation area based on upstream grid controller signal and/or local grid constraint violations. On the other hand, the CCS is designed to coordinate all DCSs and to activate their flexible demand when the flexibility is sought for upstream grid supports and/or market requirements. First, each DCS identifies grid limit violations within its area and activates flexibilities from

This article has been accepted for publication in a future issue of this journal, but has not been fully edited. Content may change prior to final publication. Citation information: DOI 10.1109/TSG.2017.2686873, IEEE Transactions on Smart Grid

EVs/HPs within its area to solve the grid issue, if exists. If the DCS cannot solve the grid limit violations, the CCS identifies grid requirements (e.g., voltage support, thermal limit violations etc.) based on the measurement received from each DCS (strategic aggregation locations) in the network. The CCS then dispatches control signals to each DCS for regulating flexible resources (e.g., HP/EV) consumptions in their respective aggregation domains.

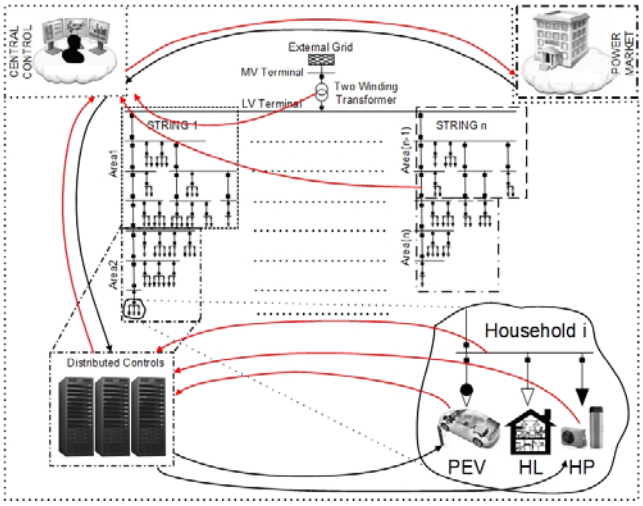

Fig. 2. Schematic representation of the hierarchical control architecture.

The proposed approach is of particular interest for short term operational planning where DSO need to understand timing, duration, location, and amount of flexibilities for solving grid constraints and/or providing supports to upstream grids. Fig. 3 illustrates a composite frame diagram for implementing the proposed HCA in DIgSILENT PowerFactory. It can be seen that each DCS monitors a voltage and power consumption from the POC of all HPs and EVs in its domain. In addition, each DCS also receives a request signal form the CCS in order to adapt the consumption according to the upstream grid requirements. On the other hand, the CCS monitors each DCS and line, and dispatches control signal to each DCS whenever grid violations are identified. As soon as any voltage violation occurs in a given area or a request is made from the CCS, the power consumption of the HPs and EVs in a particular DCS area will be regulated according to the following set of equations:

$$\begin{aligned} \Delta P_{HP}^{D\#} &= P_{HP}^{D\#} - A.P_{regHP}^{D\#} - P_{regHP}^{C\#} \\ \Delta P_{EV}^{D\#} &= P_{EV}^{D\#} - B.P_{regEV}^{D\#} - P_{regEV}^{C\#} \end{aligned} \tag{10}$$

where $\Delta P_{HP}^{D\#}$ and $\Delta P_{EV}^{D\#}$ are power consumptions to be adapted from HPs and EVs within the $\#^{th}$ DCS, $P_{HP}^{D\#}$ and $P_{EV}^{D\#}$ are their measured power consumptions at the aggregation level at $\#^{th}$ DCS, $P_{regHP}^{D\#}$ and $P_{regEV}^{D\#}$ are the power regulation required from HPs and EVs of the $\#^{th}$ DCSs in order to keep the voltage of their POCs within the stipulated limits, and $P_{regHP}^{C\#}$ and $P_{regEV}^{C\#}$ are the power regulation

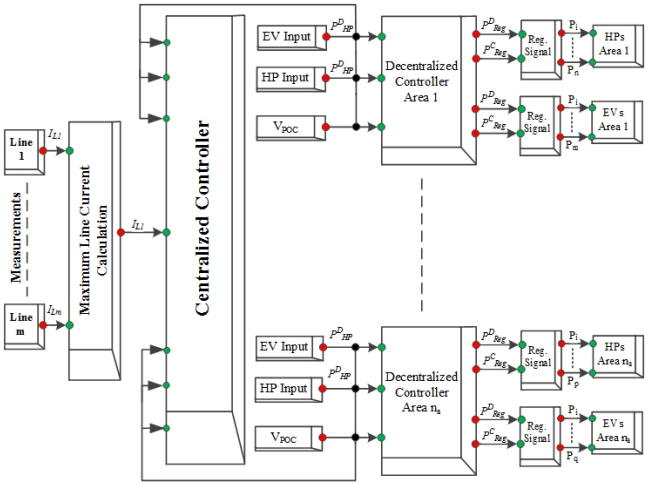

Fig. 3. Implementation of the proposed HCA in DIgSILENT PowerFactory.

required from HPs and EVs from $\#^{th}$ DCS in response to the needs of request from the CCS. Finally, A and B are the variables which define the share of the regulation power according to the instantaneous consumptions of HPs and EVs. The power regulation required from HPs and EVs within each DCS is calculated as follows:

$$\begin{aligned} P_{regHP}^{D\#} &= \int_{P_{HP}^{min}}^{P_{HP}^{max}} [k_{a1}(1-(V_{HP}^{poc}-V_{HP}^{th}))+k_{b1}(V_{HP}^{poc}-V_{HP}^{th})]dt \\ P_{regEV}^{D\#} &= \int_{P_{EV}^{min}}^{P_{EV}^{max}} [k_{a2}(1-(V_{EV}^{poc}-V_{EV}^{th}))+k_{b2}(V_{EV}^{poc}-V_{EV}^{th})]dt \end{aligned} \tag{11}$$

where k_{a1} and k_{b1} are the parameters to tune the local voltage controller affecting the consumption of the HPs and k_{a2} and k_{b2} are the respective parameters for the local voltage controller of EVs, $V_{HP}^{poc}/V_{EV}^{poc}$ is the voltage at the POC of the HP/EV, V_{HP}^{th}/V_{EV}^{th} is the threshold stipulated by the DSO, and $P_{HP}^{min}/P_{EV}^{min}$ and $P_{HP}^{max}/P_{EV}^{max}$ are minimum and maximum limits for HPs/EVs in the respective aggregation area. In particular, the upper bounds (i.e., $P_{HP}^{max}/P_{EV}^{max}$) dynamically change according to operating points of HPs/EVs, therefore computed as a difference between the rated powers and measured power at the contemporary operating points of HPs/EVs. However, since HPs cannot feed power back to grid, and only grid-to-vehicle is considered in case of EVs, the lower bounds (i.e., $P_{HP}^{min}/P_{EV}^{min}$) are set to zero.

The tuning parameters (i.e., k_{a1}, k_{b1}, K_{a2}, k_{b2}) are basically used to get proper response time and amount of flexibility activation from the EVs/HPs. In fact, the controller is designed such that those two terms add up together when the POC voltage goes below the threshold $(i.e., (V^{POC}\text{-}V^{th} \leq 0))$, thereby giving faster response to avoid anticipated voltage violations. On the other hand, when the voltage comes back to the acceptable limits $(i.e., (V^{POC}\text{-}V^{th} > 0)$, the first term opposes the second term, thereby giving comparatively slower response to progressively decrease the amount of activated flexibility. This is basically used to avoid the voltage oscillation around the V^{th} that may occur due to fast activation-deactivation of flexible resources. It should be noted that those

This article has been accepted for publication in a future issue of this journal, but has not been fully edited. Content may change prior to final publication. Citation information: DOI 10.1109/TSG.2017.2686873, IEEE Transactions on Smart Grid

gains are selected as a compromise value because the higher gains will lead to an aggressive load response which might make the voltage fluctuate rapidly and affect the customer satisfaction at the end. Whereas, the lower gains make the controller too slow and will make the power consumption not to follow the voltage changes rapidly enough, which may lead to voltage violations at the end. For the given network and simulation configurations, we used k_{a1}, k_{a2}, and k_{b1}, k_{b2} as 0.01 and -0.2, respectively.

As illustrated in Fig. 3, the CCS monitors the flexible consumption among the different areas in the LV system as well as measures the loading of the power lines. In particular, the CCS calculates and defines the thermal loading of each line, and identifies the overloaded line, if exists. Whenever the loading of any line in the system is violated, the CCS calculates the total power that needs to be regulated (P^C_{reg}) to solve the overloading as follows:

$$P^C_{reg} = \int_a^b [k_{c1}(1-(L_{th}-L_{max}))+k_{d1}(L_{th}-L_{max})]dt \quad (12)$$

where k_{c1} and k_{d1} are the parameters to tune the response from the CCS, a and b are lower and upper bounds for the regulation, L_{max} is the line loading of the most loaded line in the LV network, and L_{th} is the threshold established by the DSO. Note that the lower bound $'a'$ is zero, whereas the upper bound $'b'$ is the difference between the rated maximum current and the current loading in the feeder. Finally, the CCS distributes the regulated power P^C_{reg} among the DCSs in proportion to the availability of the flexible loads at the respective DCS. In particular, the share among the DCSs is made based on instantaneous consumptions of HPs and EVs as follows:

$$P^{D\#}_{reg} = P^C_{reg}.\frac{P^{D\#}_{HP}+P^{D\#}_{EV}}{\sum_{i=1}^{N_a} P^{D\#}_{HP}+\sum_{i=1}^{N_a} P^{D\#}_{EV}} \quad (13)$$

where N_a is the total number of aggregation areas to be obtained from Section II-A. It is demonstrated from (13) that each DCS contributes to alleviate the overloading problem irrespective of the location of overloading. However, in case of voltage violations, the flexible resources within the DCS where the voltage violations occur are first executed to resolve the issue. Nonetheless, if the DCS of that particular area cannot resolve the issue, the CCS takes this as a global problem and solves by requesting the DCSs to regulate additional power.

IV. Implementation

A. Simulation Configuration

The performance of the proposed method is demonstrated by means of a 24 hours time-sweep simulation performed in a model of a 0.4kV, 400kVA residential distribution network as shown in Fig. 4. The test network is a real-world distribution network located in the south-east of Denmark and owned by Danish DSO SEAS-NVE. One notable attribute of the proposed network is that it already has significant penetration of flexible loads, including EVs, HPs, and electric water heaters (EWHs). In fact, 50% of the consumers have HPs, 5% has EVs, and 40% has EWHs installed. The DSO anticipates some challenging issues especially in terms of under-voltage towards the end of the feeder. Therefore, this network reflects operational scenario of the real-world distribution feeder and provides an opportunity to address upcoming grid limit violations managements through the use of flexible resources. The key technical parameters of the test network are depicted in Table I.

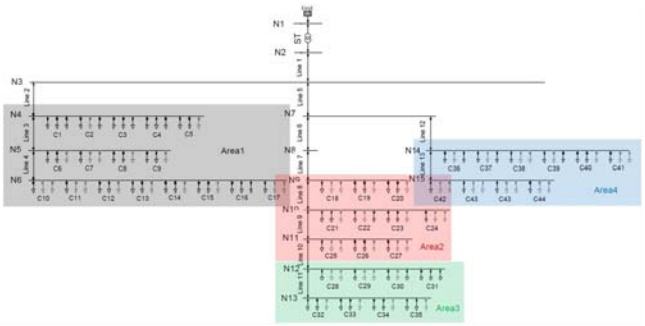

Fig. 4. Single line diagram of the test network.

A maximum demand profile over a year is taken to simulate the worst case in terms of supporting additional loads by the feeder. The impact of new electrical load penetrations to the existing network is emulated by considering 25% EV and 50% HP penetrations, that is to say, 25% and 50% of the consumers have EV and HP, respectively. The EV and HP penetrations are chosen so as to sufficiently stress the test network.

TABLE I
Key Technical Parameters of the Test Network.

Equipment	Rating	R/X
Transformer	400kVA, 19.5/0.42kV	4.64/18.64 mΩ
Network cables	335 A	207/78 mΩ/km

B. Stochastic generation of demand profiles of HPs and EVs

Generation of power consumption profiles for the individual HPs and EVs are computed using a methodology as depicted in Fig. 5. First, the consumption profiles (thermal consumptions of HPs and driving profiles of EVs) are collected for different HP and EV types. Next, a probabilistic and stochastic procedure is used to compute unit characteristics of the individual HPs and EVs. After defining corresponding parameters (e.g., power rating, thermal storage tank size etc.) that are required for the mathematical models, HPs and EVs are randomly assigned in the network. Next, the individual model parameters and input profiles are employed in the linear models as proposed in our previous work [43] to generate the electrical consumption profiles of each HP and EV. Finally, the individual consumption profiles of all HPs and EVs within each area are aggregated at the given aggregation locations.

This article has been accepted for publication in a future issue of this journal, but has not been fully edited. Content may change prior to final publication. Citation information: DOI 10.1109/TSG.2017.2686873, IEEE Transactions on Smart Grid

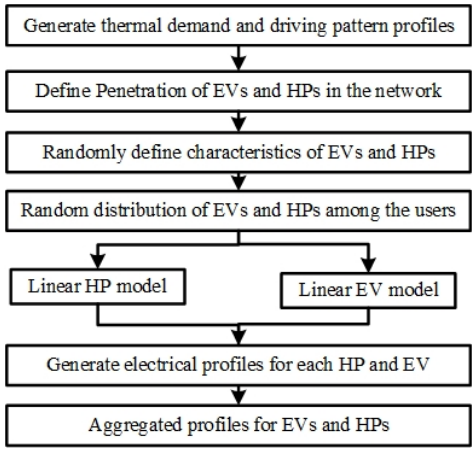

Fig. 5. Generation of power profiles of individual and aggregated HPs/EVs.

C. Case Studies

The effectiveness of the proposed methods is demonstrated by the simulation of the following three operational cases.

Case I: Case I evaluates the effectiveness and accuracy of the aggregated network model compared to the detailed network performance.

Case II: This case demonstrates effectiveness of the proposed control mechanism when each DCS acts over the aggregated flexible demand of their specific area to solve local grid limit violations.

Case III: It intends to demonstrate the effectiveness of the CCS to exploit aggregated flexible demand of each aggregated area to solve global network problems.

D. Computational Environment

This study was performed using DIgSILENT PowerFactory and MATLAB. The DIgSILENT was used for dynamic simulation whereas MATLAB was used for the computation, including GA based optimization and network reduction. The framework utilized for performing the necessary dynamic simulations for validating the entire control approach is made in DIgSILENT Powerfactory 15.2 on Windows-7 machine having 64-bit operating system, 2.3 GHz processor, and 4 GB RAM. The average time for running a 24 hours time-sweep simulation with a step size of 0.1 second for the detailed model was observed to be between 8 to 10 minutes, whereas it took 50 to 70 seconds to run the 24 hours time sweep simulation of the aggregated (i.e., reduced) network. The aggregated model is computationally less demanding, thereby helping the DSOs to take faster operational decisions. It is worth mentioning that the planning related decision, including GA based optimization, network reduction, and profile generation for HPs and EVs were done using MATLAB 2013a on the same machine. The observed time for GA optimization was 5 to 13 minutes while running with different population size and crossover/mutation rates.

V. Simulation Results and Discussion

A. Optimum Aggregation and Network Reduction

As mentioned in Section II-A, optimum aggregation areas for the given network are computed by minimizing the total cost of aggregation and sum of distances between consumers and aggregation points. The optimization algorithm results in aggregation areas and aggregation points as illustrated in Table II. For the given test network, it can be clearly seen that the optimization results in four aggregations areas (Area-1 through Area-4). The strategic locations for the corresponding aggregation areas are at nodes 5, 10, 12, and 14 of the non aggregated network. One notable attribute is that nearby nodes that are served by the same feeder or lateral are aggregated together. This is of particular importance as the aggregation of consumers served by different sub-feeders may complicate the observability and controllability of the aggregated area.

TABLE II
Aggregation results based on GA available in MATLAB.

Description	Nodes	Strategic Aggregation Point
Aggregation Area-1	[4, 5, 6]	Node-5
Aggregation Area-2	[9, 10, 11]	Node-10
Aggregation Area-3	[12, 13]	Node-12
Aggregation Area-4	[14, 15]	Node-14

After aggregation, the original test network is reduced to an equivalent aggregated network having the four aggregated nodes as shown in Fig. 6. This is of key importance as the simplified equivalent network facilitates DSOs to make faster operational decisions regarding better utilization of the available flexibility. As grid solutions (e.g., power flow, state estimation) of larger distribution grids are time consuming and computationally challenging, the reduced network provides an excellent tool when faster decisions are desired. However, the key challenge is to determine the aggregated load and the equivalent line impedances for each aggregated area (i.e., lines 2, 4, 5, and 6 as shown in Fig. 6).

As aggregated power and equivalent line impedances are function of load variations, the power consumption is first clustered into the given N_c. Subsequently, the clustered power is utilized to compute aggregated loads and equivalent line impedances by using circuit reduction approach. In particular, one year (March 2012 through February 2013) of hourly consumption data for the test network are clustered into three clusters using hierarchical clustering approach. Fig. 7a) illustrates the aggregated power and Fig. 7b) illustrates association of the each hour of the day to the corresponding clusters. It can be observed from Fig. 7 that the variations in power consumptions over a day are a function of clusters, such that any daily/seasonal variations on load profiles are reflected in terms of difference in power. In particular, a higher cluster number reflects higher power consumptions and vice-versa. That is to say, cluster-2 has higher power consumption than cluster-1, and cluster-3 has higher power consumption than cluster-1 and cluster-2.

This article has been accepted for publication in a future issue of this journal, but has not been fully edited. Content may change prior to final publication. Citation information: DOI 10.1109/TSG.2017.2686873, IEEE Transactions on Smart Grid

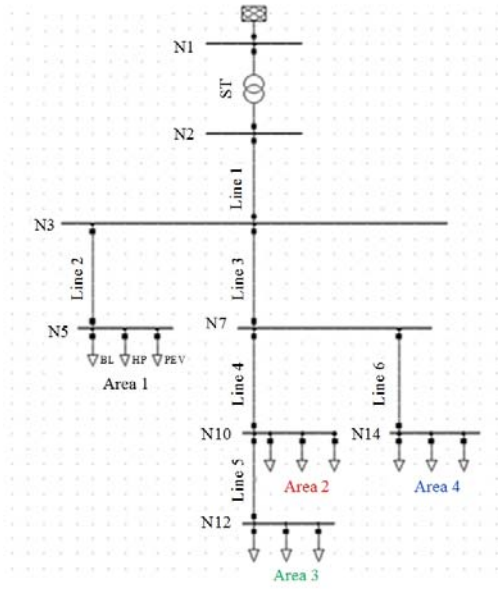

Fig. 6. Simplified reduced (aggregated) network.

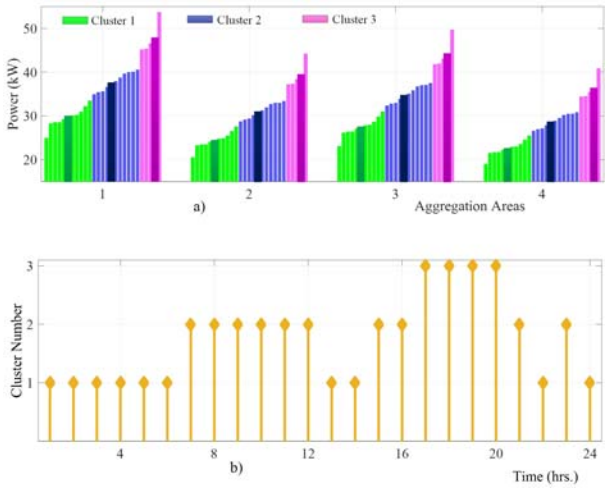

Fig. 7. a) Power variation per aggregation area and b) Clustering of hourly consumption.

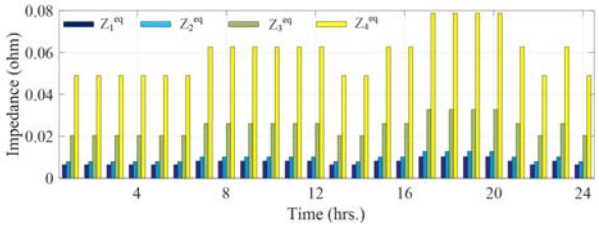

Fig. 8. Variation of equivalent impedance over a day in future grid scenario.

Fig. 8 illustrates the equivalent upstream impedances of each aggregation area. It can be seen that the equivalent impedance of each aggregated area is a function of time and vary significantly among the aggregation areas. The relative differences in equivalent impedances among the aggregation areas are due to difference in line impedance of the upstream feeding line to each area. However, the temporal differences in the equivalent impedance arise due to random allocation and consumptions of the EVs and HPs. It is worth mentioning that even though the equivalent impedance of each aggregation area changes dynamically, assessment of the aggregated network is performed by taking only highest impedance values of the corresponding area. This is done to demonstrate the worst case network performance.

B. Control Implementation

This section demonstrates the performance of the proposed method by simulating the following three cases.

1) Case I: This case is used to demonstrate the performance of the aggregated network model and its comparison with the detailed (non-aggregated) version. Fig. 9 illustrates the simulation results of Case I, where Fig. 9(a) is the loading of the secondary transformer (ST), Fig. 9(b) is the total active power consumption of base load (BL), EVs, and HPs, Fig. 9(c) is the aggregated active power consumption for the BL per aggregation area, Fig. 9(d) is the aggregated active power consumption for the HPs per aggregation area, Fig. 9(e) is the aggregated active power consumption for the EVs per aggregation area, Fig. 9(f) is the loading of the highly loaded power line in the LV network, and Fig. 9(g) is the minimum voltage in the LV network. Please note that this case study is intended to demonstrate performance of the aggregated network with respect to the detailed one. Therefore, the performance is investigated without implementing any control.

It can be observed that the given penetration level of HPs and EVs, illustrated in Fig. 9(c) and Fig. 9(d), significantly stresses the test network during the peak periods. As shown in Fig. 9(b), the power consumptions from EVs and HPs is significant in comparison with the BL, which is significant enough to congest the network. In fact, such penetration forces the network towards voltage and current limits violations. Looking into Fig. 9(f) and Fig. 9(g), the nature of the bottleneck is under-voltage during 18:00 through 20:00 in bus N_{12} of the aggregated network. Moreover, Line-1, the highest loaded line in the network, is overloaded in the peak periods. Note that 80% or higher loading is considered as overloading in this study.

Loading of the highest loaded line and the voltage profile of the voltage at the minimum voltage node for aggregated (red) and non-aggregated (black) networks are depicted in Fig. 9(f) and 9(g), respectively. It can be seen that both the minimum voltage and maximum loading are pretty much the same for both aggregated and non-aggregated networks. However, very small difference can be observed between them. This is especially relevant in Fig. 9(g) where the voltage profile of the aggregated network is slightly elevated compared to the non-aggregated. Nevertheless, the error is quite small, which can be negligible for DSOs to make operational planning decisions.

This article has been accepted for publication in a future issue of this journal, but has not been fully edited. Content may change prior to final publication. Citation information: DOI 10.1109/TSG.2017.2686873, IEEE Transactions on Smart Grid

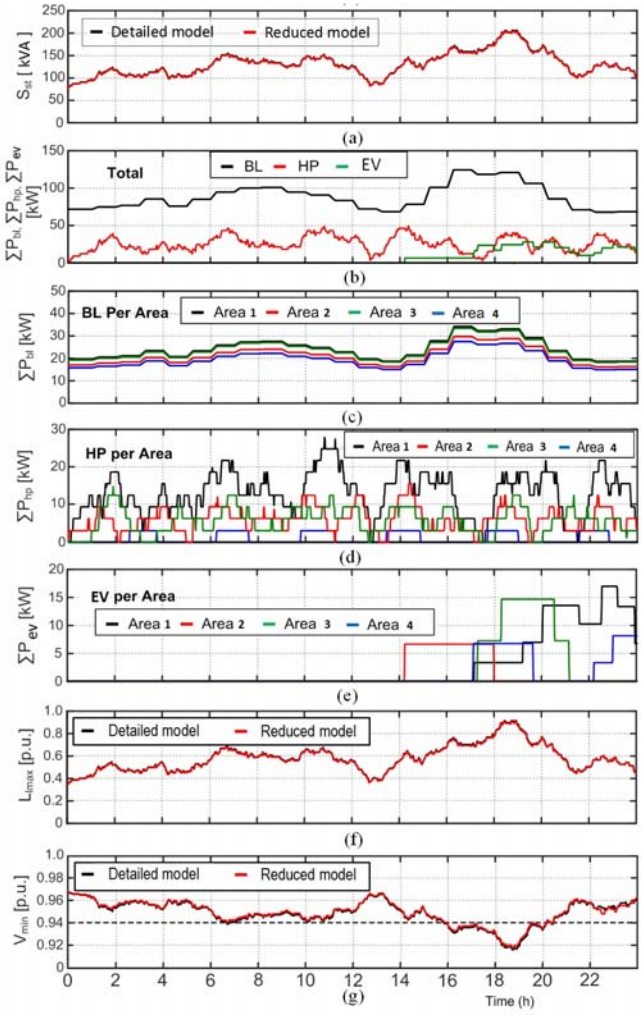

Fig. 9. Case I: (a) Loading of ST (b) Aggregated active power consumption at ST, (c) Aggregated active power consumption of BL EV, and HP per area, (d) Aggregated active power consumption of HPs per area, (e) Aggregated active power consumption of EVs per area, (f) Loading of maximum loaded line in the grid, (g) Minimum voltage in the grid.

From the observation of minimum voltage (Fig. 9(g)), maximum loading (Fig. 9(f)), and total loading at the substation (Fig. 9(a)), we can say that the reduced network follow the detailed network pretty well with very low errors. In fact, the observed error is less than 1% in minimum voltage, which is fairly accurate for DSOs to make operational planning. More importantly, the reduced network significantly reduces the computational burdens. For instance, the computation of aggregated network took approximately 50 seconds compared to approximately 9 minutes for the detailed network.

2) Case II: This case demonstrates the effectiveness of the proposed DCS control strategy in solving local voltage problems in the network, and compares the performance with and without control scenarios. Fig. 10 illustrates the simulation results of Case II when DCSs are used to solve a local voltage problems in their respective area. In particular, Fig. 10(a) is the loading of the ST, Fig. 10(b) is the total consumption of BL, EVs, and HPs, Fig. 10(c) is the HP consumption per aggregation area, Fig. 10(d) is EV consumption per aggregation area, Fig. 10(e) is the loading of the maximum observed loading, Fig. 9(f) is the minimum observed voltage, Fig. 10(g) is the total power regulated from each DCS. Please note that all the plots in Fig. 10 reflect with and without control of the flexible loads (i.e., EVs/HPs).

Whenever an under-voltage situation originates at any node, the DCS which is responsible for the corresponding node adjusts the power consumptions of the EVs and HPs to bring the voltage back to the limit. For instance, followed by the voltage violations at bus N_{12} of the aggregated network, which is in "Area-3", the DCS responsible for this area modifies the power consumption of HPs and EVs in that area as shown in Fig. 10(g) and bring the voltage above the threshold voltage illustrated by dotted line. In fact, the voltage improvement was realized by the reduction in regulating power as shown in Fig. 10(a). For the given configuration, the power regulation from DCS is observed to be approximately 26 kW during the peak period.

It can be seen from Fig. 10(g) that DCS of Area-3 contributes the most to solve the under-voltage, whereas the DCSs of some areas are not contributing at all to support the voltage. This is further demonstrated by illustrating the actual power regulations of EVs and HPs in each aggregation area are depicted in Fig. 11(c) and Fig. 10(d), respectively. One notable attribute is that other DCSs which are supplied by the same feeder also contribute to the voltage support provided voltage of at least one node whithin that DCS gets violated. For instance, as shown in Fig. 10(g), the aggregation area-2 which is upstream to area-3 also contributes in response to the under-voltage observed in area-3. In fact, the area wise contributions of HPs and EVs are demonstrated in Fig. 10(c) and Fig. 10(d), respectively. Note that the contribution of upstream DCS to solve the downstream voltage violations is ensured by setting slightly higher threshold voltage for the upstream area than for the downstream area. Such strategy is effective in sharing voltage support responsibility among the DCSs in different areas in order not to always penalize the same DCS, for instance the DCS towards the end of the feeder.

3) Case III: This case demonstrates the performance of the CCS in resolving the grid constraints, particularly thermal overloading, in the network. Fig. 11 illustrates the simulation results of Case III, where Fig. 11(a) through Fig. 11(f) are same as the case II, while Fig. 11(g) represents the power requested by the CCS to each DCS. Unlike Case-II which only considers DCS, this case also considers the contribution of CCS in addressing the overloading. For the given network, voltage violations occurs before thermal overloading. Therefore, we set 70% line loading as thermal limits for each line. Such setting was done to force the CCS to react to the violations before DCSs are triggered by the local voltage violations. As such the simulation illustrates the effectiveness of the CCS in solving global (network level) problems; particularly thermal overloading. The thermal threshold enables the CCS to

This article has been accepted for publication in a future issue of this journal, but has not been fully edited. Content may change prior to final publication. Citation information: DOI 10.1109/TSG.2017.2686873, IEEE Transactions on Smart Grid

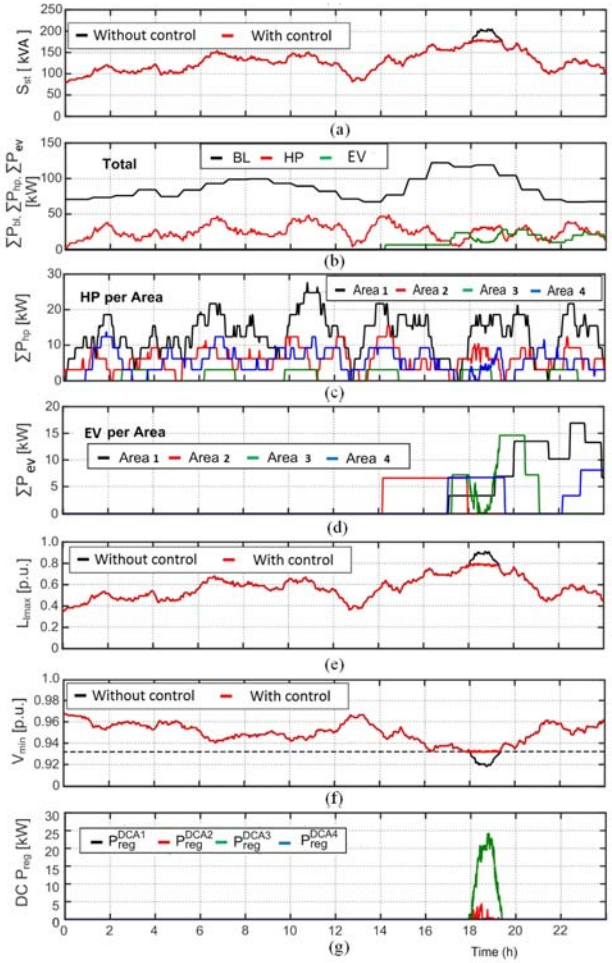

Fig. 10. Case II: (a) Loading of ST (b) Aggregated active power consumption at ST level, (c) Aggregated active power consumption of HPs per area, (d) Aggregated active power consumption of EVs per area, (e) Loading of maximum loaded line in the grid, (f) Minimum voltage in the grid, (g) Regulation power required from each DCS.

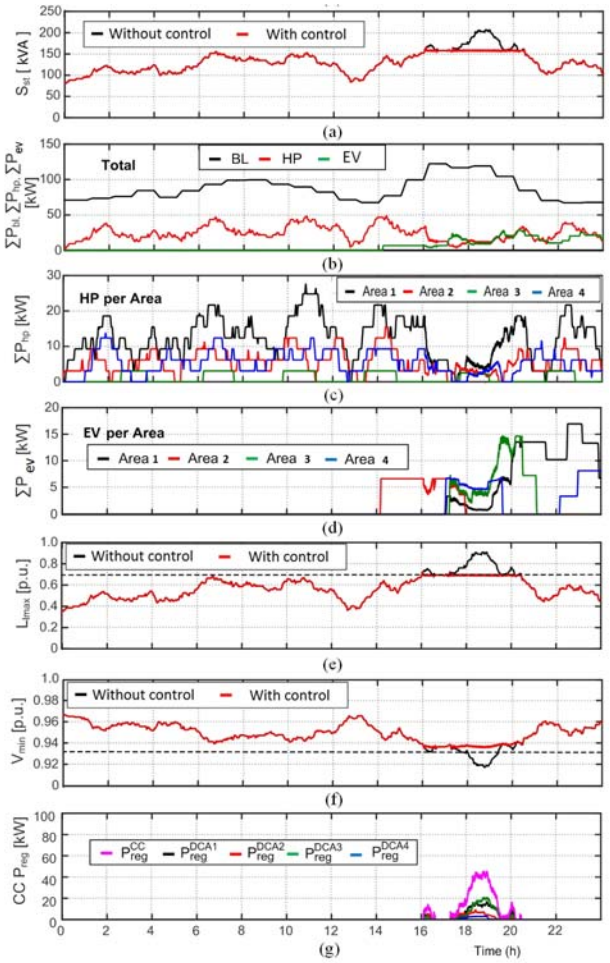

Fig. 11. Case III: (a) Loading of ST (b) Aggregated active power consumption at ST level, (c) Aggregated active power consumption of HPs per area, (d) Aggregated active power consumption of EVs per area, (e) Loading of maximum loaded line in the grid, (f) Minimum voltage in the grid, (g) Regulation power required from the CCS to each DCS.

identify overload issues before DCS detect any under-voltage limit violation in its zone.

For the proposed simulation case, the voltages of none of the nodes in controlled mode never reach to the threshold voltage (set as dotted line) in Fig. 11(g). Therefore, DCSs are triggered only by the CCS in this case rather than the local voltage violations. However, it is clear that maximum loading limit is violated in the main line as shown by dotted line in Fig. 11(e). Therefore, the CCS senses it and accordingly request to regulate power from all DCS in the LV system to solve the overloading. As illustrated in Fig.11(g), the amount of regulating power requested from each DCSs varies significantly. This is due to differences in sizes of aggregation area, and penetration levels and power consumption capacities of HPs and EVs among the aggregated areas. In fact, 11(c) and Fig. 11(d) demonstrates the variation in total power consumptions from HPs and EVs from different aggregation areas. It can be observed that the power consumption of area-1 and area-3 are larger compared to the others. This also contributes to the variation in flexibility contribution from different area. For the given simulation configuration, the peak of regulation power which is requested by the CCS is given between the 18 and 20 hours and is about 45 kW.

VI. Conclusion

This study proposed an algorithm to compute optimum aggregation of spatially distributed flexible resources in a power distribution network considering geographical sparsity of the resources and cost associated with the aggregation. In addition, a hierarchical control architecture provided with a combination of centralized and decentralized control was designed not only to deploy the aggregated flexibilities for solving local grid constraint violations, but also to facilitate trading of small distributed resources to different power and energy markets. The architecture also serves as a great operational tool for DSOs in better utilization of the available flexibilities for

supporting electrical grids. The simulation studies performed for three operational scenarios demonstrated that this method can greatly helps DSOs in deciding the need of exact amount of flexibilities from specific network section(s) in solving particular grid constraints or fulfilling grid requirements. For the given configuration, the performance of the aggregated model is very close to the that of the non-aggregated network, thereby demonstrating the accuracy of the proposed method.

REFERENCES

[1] The U. S. Department of Energy, "Smart grid system report," *Technical Report*, Aug. 2014.

[2] Danish Energy Association, "Energinet.dk, smart grid in denmark 2.0," *Technical Report*, 2010.

[3] H. Mohsenian-Rad, "Optimal demand bidding for time-shiftable loads," *IEEE Trans. on Power System*, vol. 30, pp. 939-951, Jul. 2014.

[4] C. O. Adika and L. Wang, "Demand-Side Bidding Strategy for Residential Energy Management in a Smart Grid Environment," *IEEE Trans. on Smart Grid*, vol. 5, no. 4, pp. 1724-1733, Jul. 2014.

[5] A. Molina-Garcia, F. Bouffard, and D. S. Kirschen, "Decentralized Demand-Side Contribution to Primary Frequency Control," *IEEE Trans. on Power Systems*, vol. 26, pp. 411-419, Feb. 2011.

[6] R. Yu, et. al., "Balancing power demand through EV mobility in vehicleto-grid mobile energy networks," *IEEE Trans. on Industrial Informatics*, vol. 12, pp. 79-90, 2016.

[7] M. Parvania and M. Fotuhi-Firuzabad, "Demand response scheduling by stochastic SCUC," *IEEE Trans. on Smart Grid*, vol. 1, pp. 89-98, Jun. 2010.

[8] B. P. Bhattarai, M. Levesque, B. Bak-Jensen, J. R. Pillai, M. Maier, D. Tipper, and K. S. Myers, "Design and co-simulation of hierarchical architecture for demand resonse control and coordination," *IEEE Trans. on Industrial Informatics* (Early Access), 2016.

[9] E. L. Karfopoulos, K. A. Panourgaias, and N. D. Hatziargyriou, "Distributed coordination of electric vehicles providing V2G regulation services," *IEEE Trans. on Power Systems*, vol. 31, pp. 2834-2846, 2016.

[10] O. Kilkki, A. Alahaivala, and I. Seilonen, "Optimized control of price based demand response with electric storage and space heating," *IEEE Trans. on Industrial Informatics*, vol. 11, pp. 281-288, Feb. 2015.

[11] K. Christakou, D. Tomozei, J. L. Boudec, and M. Paolone, "GECN: Primary voltage control for active distribution networks via real-time demand response," *IEEE Trans. on Smart Grid*, vol. 5, pp. 622-631, Mar. 2014.

[12] K. H. Nunna, and S. Doolla, "Responsive end-user-based demand side management in multi-microgrid environment", *IEEE Trans. on Industrial Informatics*, vol. 10, pp. 1262-1272, May 2014.

[13] C. Eid, P. Codani, Y. Chen, Y. Perez, and R. Hakvoort, "Aggregation of demand side flexibility in a smart grid: A review for European Market Design," In Proc. *EEM15*, May, 2015.

[14] B. Biegel, L. H. Hansen, J. Stostrup, P. Andersen, and S. Harbo, "Value of flexible consumption in the electricity markets," *Energy*, vol. 66, pp. 354-362, 2014.

[15] K. Kouzelis, Z. H. Tan, B. Bak-Jensen, P. Mahat, J. R. Pillai, "A Simplified Short Term Load Forecasting Method Based on Sequential Patterns," In Proc. *IEEE ISGT-Europe*, 2014.

[16] P. Dievel, F. Vos, and R. Belmans, "Demand response in electricity distribution grids: Regulatory framework and barriers," In Proc. *EEM*, 2014.

[17] B. P. Bhattarai, M. Lvesque, M. Maier, B. Bak-Jensen, J. R. Pillai, "Optimizing Electric Vehicle Coordination Over a Heterogeneous Mesh Network in a Scaled-Down Smart Grid Testbed," *IEEE Trans. on Smart Grid*, vol. 6, pp. 784-794, 2015.

[18] B. P. Bhattarai, B. Bak-Jensen, J. R. Pillai, P. Mahat, "Two-Stage Electric Vehicle Charging Coordination in Low Voltage Distribution Grids," In Proc. *IEEE APPEEC*, Dec. 2014.

[19] P. Mirowski, S. Chen, T. K. Ho, C. Yu, "Demand forecasting in smart grids," *Bell Labs Technical Journal*, vol 18, no 4, March, 2014.

[20] B. P. Bhattarai, B. Bak-Jensen, P. Mahat, J. R. Pillai, M. Maier, "Hierarchical Control Architecture for Demand Response in Smart Grid Scenario," In Proc. *IEEE PES APPEEC*, pp. 1-6, Dec. 2013.

[21] I. A. Sajjad, G. Chicco, and R. Napoli, "Definitions of demand flexibility for aggregate residential loads," *IEEE Trans. on Smart Grid*, vol. 7, pp. 2633-2643, 2016.

[22] S. A. Saleh, P. Pijnenburg, and E. Castillo-Guerra, "Load aggregation from generation-follows-load to load-follows-generation: Residential loads," *IEEE Trans. on Industry Applications*, Early Access (DOI 10.1109/TIA.2016.2626261).

[23] B. P. Bhattarai, B. Bak-Jensen, J. Pillai, M. Maier, "Demand flexibility from residential heat pump," In Proc. *IEEE PES GM*, 2014.

[24] H. Hao, B. Sanandaji, K. Poola, "Aggregate flexibility of thermostatically controlled loads," *IEEE Trans. on Power System*, vol 30, Jan 2015.

[25] S. Mhanna, A. C. Chapman, G. Verbic, "A fast distributed algorithm for large scale demand response aggregation," *IEEE Trans. on Smart Grid*, vol. 7, pp. 2094-2107, 2016.

[26] S. Mhanna, G. Verbic, A. C. Chapman, "A faithful distributed mechanism for demand response aggregation," *IEEE Trans. on Smart Grid*, vol. 7, pp. 1743-1753, 2016.

[27] M. Parvania, M. Fotuhi-Firuzabad, and M. Shahidehpour, "Optimal demand response aggregation in wholesale electricity market," *IEEE Trans. on Smart Grid*, vol. 4, pp. 1957-1965, 2016.

[28] J. Zhang and A. D. Dominguez-Garcia, "Evaluation of demand response resource aggregation system capacity under uncertainty," *IEEE Trans. on Smart Grid*, Early Access (DOI 10.1109/TSG.2017.2663780).

[29] J. Hoog, et. al., "Electric vehicle charging and grid constraints: comparing distributed and centralized approaches," In Proc. *IEEE PES GM*, pp. 1-5, 2013.

[30] P. Richardson, D. Flynn, and A. Keane, "Local versus centralized charging strategies for electric vehicles in low voltage distribution systems," *IEEE Trans. on Smart Grid*, vol. 3, pp. 1020-1028, Jun. 2012.

[31] B. P. Bhattarai, B. Bak-Jensen, P. Mahat, J. R. Pillai, "Voltage Controlled Dynamic Demand Response," In Proc. *IEEE ISGT*, 2013.

[32] S. Lu, et. al., "Centralized and decentralized control for demand response," In Proc. *IEEE PES ISGT*, pp. 1-5, 2011.

[33] T. L. Vandoom, et. al., "Microgrids: hierarchical control and an overview of the control and reserve management strategies," *IEEE Industrial Electronics Magazine*, vol. 7, no. 4, pp. 42-55, Dec. 2013.

[34] V. Bui, A. Hussain, and H. Kim, "A multiagent-based hierarchical energy management strategy for multi-microgrids considering adjustable power and demand response," *IEEE Trans. on Smart Grid*, 2016.

[35] G. R. Bharati and S. Paudyal, "Coordinated control of distribution grid and electric vehicle loads," *Electric Power Systems Research*, vol. 140, pp. 761-768, Nov. 2016.

[36] B. P. Bhattarai, B. Bak-Jensen, J. R. Pillai, J. Gentle, K. Myers, "Overvoltage mitigation using coordinated control of demand response and grid-tiled rooftop photovoltaic," In Proc. *IEEE SusTech*, 2015.

[37] E. Mocanu, P. Nguyen, M. Gibescu, "Energy disaggregation for real-time building flexibility detection," In Proc. *IEEE PES GM*, 2016.

[38] S. Paudyal, C. A. Canizares and K. Bhattacharya, "Three-phase distribution OPF in smart grids: Optimality versus computational burden," 2nd IEEE PES Innovative Smart Grid Technologies, Manchester, 2011.

[39] J. Kwac, J. Flora, and R. Rajagopal, "Household energy consumption segmentation using hourly data," IEEE Trans. on Smart Grid, vol. 5, no. 1, pp. 420-430, Jan. 2014.

[40] G. Chicco, R. Napoli, and F. Piglione, "Comparisons among Clustering Techniques for Electricity Customer Classification," IEEE Trans. on Power System, vol. 21, no. 2, pp. 933-940, May 2006.

[41] K. Kouzelis, Z. Tan, B. Bak-Jensen, J. Pillai, and E. Ritchie, "Estimation of Residential Heat Pump Consumption for Flexibility Market Applications," *IEEE Trans. Smart Grid*, vol. 6, pp. 1852-1864, 2015.

[42] H. Ahmadi, J. R. Mart, and H. W. Dommel, "A Framework for Volt-VAR Optimization in Distribution Systems," *IEEE Trans. Smart Grid*, vol. 6, pp. 1473-1483, 2015.

[43] I. D. Mendaza, A. Pigazo, B. Bak-Jensen, Z. Chen, "Generation of domestic hot water, space heating and driving pattern profiles for integration analysis of active loads in low voltage grids,", In Proc. *IEEE ISGT*, 2013.

This article has been accepted for publication in a future issue of this journal, but has not been fully edited. Content may change prior to final publication. Citation information: DOI 10.1109/TSG.2017.2686873, IEEE Transactions on Smart Grid

Bishnu P. Bhattarai (S'12-M'16) received his M.Sc. in Power System Engineering from Tribhuvan University, Nepal and Osaka Sangyo University, Japan, in 2010 and Ph.D. in Energy Technology from Aalborg University, Denmark in 2015. He is currently working on various aspects of microgrid and cyber-physcal security of the electrical infrastructure at Idaho National Laboratory, Idaho, USA. He was a visiting scholar at Institut National de la Recherche Scientifique (INRS), Montreal, Canada, where he demonstrated power and communication aspects of smart grid through development of scaled-down smart grid testbed. He was the recipient of Nepal government's prestigious award 'Nepal Vidya Bhusan' awarded by the President of Nepal for his best performance during graduate studies. His current research interests include grid integration of renewables, smart energy system, cyber-physical security of grid infrastructure, demand response, grid resiliency, and dynamic line rating.

Iker Diaz de Cerio Mendaza (M'11) received the B.Eng. degree in electrical engineering, and the M.Eng. degree in industrial engineering and renewable energy from the University of the Basque Country, Leioa, Spain, in 2007 and 2009, respectively; the M.Sc. degree in industrial engineering and renewable energy from the University of Zaragoza, Zaragoza, Spain, in 2010; and the Ph.D. degree in electrical engineering from Aalborg University, Aalborg, Denmark, in 2014. From 2010 to 2011, he was a Project Engineer with WindVision Ltd., Leuven, Belgium. He is currently working as a planning engineer at Energinet.dk. His current research interests include demand response, smart grids, and active distribution networks.

Kurt S. Myers (M'15) is a Project Manager and Staff Electrical Engineer at Idaho National Laboratory, Idaho, USA. He received the B.Sc. degree in physics from the University of Washington in 1992 and the M.Sc. degree in electrical engineering from Washington State University in 1997. He has more than 20 years of experience at the laboratory working with multiple government, industry, and university collaborators. He has authored many technical papers, reports, articles, and presentations on wind and solar power, electrical engineering, and power systems. He is also a licensed Professional Engineer in the State of Idaho.

Birgitte Bak-Jensen (SM'12) received her M.Sc. degree in Electrical Engineering in 1986 and a Ph.D. degree in Modelling of High Voltage Components in 1992, both from Institute of Energy Technology, Aalborg University, Denmark. From 1986-1988, she was with Electrolux Elmotor A/S, Aalborg, Denmark as an Electrical Design Engineer. She is now Professor in Intelligent Control of the Power Distribution System at the Institute of Energy Technology, Aalborg University. Her fields of interest are mainly related to the operation and control of the distribution grid including power quality and stability in power systems and taking integration of dispersed generation and smart grid issues like demand response into account. Also the interaction between the electrical grid and the heating and transport sector is a key area of interest.

Sumit Paudyal (S'7-M'13) received the Bachelors degree from Tribhuvan University, Kathmandu, Nepal, in 2003; the M.Sc. degree from the University of Saskatchewan, Saskatoon, SK, Canada, in 2008; and the Ph.D. degree from the University of Waterloo, Waterloo, ON, Canada, in 2012, all in electrical engineering. He joined the Department of Electrical and Computer Engineering, Michigan Technological University, Houghton, MI, USA, as an Assistant Professor, in 2012. He was a Research Assistant with Kathmandu Engineering College, Kathmandu, in 2003, and an Electrical Engineer with the Nepal Electricity Authority, Kathmandu, in 2004. His current research interests include smart distribution grid operations, power system protection, power system real-time hardware simulations, and optimization techniques in power systems.